Evolutionary acquisition of a primitive light-dependent nuclear relocation in *Marchantia polymorpha*

Kosei Iwabuchi[1,*] Hiroki Yagi[2], Kenta C. Moriya[3], Aino Komatsu[4,9], Noriyuki Suetsugu[5], Yuuki Sakai[6], Tomoo Shimada[7], Ryuichi Nishihama[8], Takayuki Kohchi[9], Akiko Harada[1], Yo-hei Watanabe[2], Haruko Ueda[2] & Ikuko Hara-Nishimura[2,*]

[1]Faculty of Medicine, Osaka Medical and Pharmaceutical University, Takatsuki 569-8686, Japan
[2]Faculty of Science and Engineering, Konan University, Kobe 658-8501, Japan
[3]Center for Ecological Research, Kyoto University, Otsu 520-2113, Japan
[4]Graduate School of Life Sciences, Tohoku University, Sendai 980-8577, Japan
[5]Graduate School of Arts and Sciences, The University of Tokyo, Tokyo 153-8902, Japan
[6]Graduate School of Science, Kobe University, Kobe 657-8501, Japan
[7]Graduate School of Science, Kyoto University, Kyoto 606-8502, Japan
[8]Faculty of Science and Technology, Tokyo University of Science, Noda 278-8510, Japan
[9]Graduate School of Biostudies, Kyoto University, Kyoto 606-8502, Japan

[*]Correspondence should be addressed to K. I. (e-mail: kosei.iwabuchi@ompu.ac.jp) and I. H.-N. (e-mail: ihnishi@gr.bot.kyoto-u.ac.jp).

ORCID IDs: 0000-0002-3696-6806 (K.I.), 0000-0001-8814-1593 (I.H.-N.)

Abstract

***Arabidopsis thaliana* is known to position nuclei on the bottom wall of leaf cells, distancing genetic material from external stresses, and, in response to intense blue light, it relocates them to the side walls to escape UV-induced DNA damage[1]. However, how this protective system evolved in land plants remains unclear. Here, we show that *Chara corallina*, the charophyte alga, has no light-dependent nuclear relocation and that *Marchantia polymorpha*, a modern relative of the earliest land plants, has a nuclear positioning system distinct from that of Arabidopsis: it positions nuclei on the upper walls of the epidermal cells of the young thalli in the dark and even in prolonged intense light. We also show that, in response to intense blue light, *M. polymorpha* has the ability to immediately move nuclei from the upper to the side walls in an actin filament-dependent manner similarly to Arabidopsis. However, the relocation is transient and the nuclei return to the upper walls depending on two cytoskeletal components (actin filaments and microtubules). Together, these findings suggest that light-dependent nuclear relocation was initially established in bryophytes and then diverged as land plants evolved.**

Light-dependent nuclear relocation does not occur in charophyte algae (Extended Data Fig. 1), where nuclei move dynamically along the cytoplasmic streaming, but does occur in a pteridophyte fern[2-4] and a flowering plant[5]. We investigated whether nuclear positioning exists in the liverwort by focusing on epidermal cells near the apical notches of the young thalli (called gemmalings) of *M. polymorpha* (Extended Data Fig. 2). In the dark, *M. polymorpha* positioned the nuclei on the upper walls of the cells (Fig. 1a, arrowheads), in contrast to their positioning on the bottom walls of leaf cells in Arabidopsis[5]. For quantitative analysis, nuclei were categorized into three positions: upper walls, side walls, and bottom walls (Fig. 1b). More than 90% of the nuclei were positioned on the upper walls with almost no nuclei positioned on the bottom walls (Fig. 1c, wild type).

Unexpectedly, under the artificial condition of continuous exposure to low light for 3 days, 75% of the nuclei were positioned on the side walls (Fig. 1d, arrowheads; see below for detailed mechanism). To examine relocation of the nuclei, we transferred gemmalings with

nuclei on the side walls to the dark. Most of the nuclei relocated to the upper walls after 0.5 days of dark treatment, and remained there (Fig. 1e). The dark-induced side-to-upper nuclear relocation was inhibited by either the actin-depolymerizing reagent latrunculin B or the microtubule-disrupting reagent oryzalin (Fig. 1f). Simultaneous treatment with both reagents significantly inhibited the relocation (Fig. 1f). These results indicate that *M. polymorpha* uses both actin and microtubule cytoskeletons for dark-induced side-to-upper nuclear relocation (Fig. 1g). In contrast, in Arabidopsis, only actin is involved in the dark-induced side-to-bottom nuclear relocation[6,7].

In Arabidopsis, nuclear relocation is associated with chloroplast movement through two proteins: CHLOROPLAST UNUSUAL POSITIONING 1 (CHUP1) [8] and KINESIN-LIKE PROTEIN FOR ACTIN-BASED CHLOROPLAST MOVEMENT1 (KAC1) [9]. Phylogenetic analysis confirmed the presence of MpCHUP1 and MpKAC in *M. polymorpha* (Extended Data Fig. 3). We examined two Mp*chup1* mutant alleles (knockout mutant Mp*chup1*^{KO} and large deletion mutant Mp*chup1*^{ld}) and two Mp*kac* mutant alleles (knockout mutant Mp*kac*^{KO} and genome editing mutant Mp*kac*^{ge}). None of the mutations resulted in significant defects in dark-induced nuclear positioning on the upper walls (Fig. 1c and Extended Data Fig. 4a), indicating that the relocation is independent of chloroplast movement. This result was supported by the imaging data in the dark (Fig. 1a) showing that the distribution of nuclei was different from that of chloroplasts.

In response to intense blue light, vascular plants relocate nuclei to the side walls and keep them there[10], thereby avoiding ultraviolet B (UVB)-induced DNA damage and cell death[1]. To examine the effect of intense light on the nuclear relocation, we irradiated dark-adapted *M. polymorpha* gemmalings with intense light (300 μmol m^{-2} s^{-1}) at various wavelengths (blue, green, red, and far-red) for 3 h. The nuclei relocated from the upper to the side walls specifically in response to blue light (Extended Data Fig. 4b). The percentage of nuclei that relocated from the upper to the side walls increased dose-dependently in the range of 50–300 μmol m^{-2} s^{-1} of blue light, but it was not more than 50% (Fig. 2d).

Surprisingly, in the presence of prolonged exposure (>3 h) to intense blue light (300 μmol m^{-2} s^{-1}), the nuclei that relocated to the side walls returned to the upper walls and remained there (Fig. 2a,b). The intense light-induced nuclear relocation of *M. polymorpha*

therefore consisted of two phases: the upper-to-side nuclear relocation within 3 h (named Phase I) followed by the side-to-upper nuclear relocation that persisted over a longer period (named Phase II). The dual-phase nuclear relocation was entirely correlated with the chloroplast movement, in which chloroplasts were relocated to the side walls and then to the upper walls (Fig. 2c).

The nuclear relocation during phase I was remarkably suppressed in all mutants of Mp*phot*^{KO}, Mp*chup1*^{KO}, Mp*chup1*^{ld}, Mp*kac*^{KO}, and Mp*kac*^{ge} (Fig. 2e and Extended Data Fig. 4c), indicating that Phase I is regulated by the blue-light photoreceptor phototropin (MpPHOT) and two chloroplast movement-related protein homologues (MpCHUP1 and MpKAC). Cytoskeletal drug analysis showed that actin filaments, but not microtubule, are involved in Phase I movements of nuclei (Fig. 2f) and chloroplasts (Fig. 2g). These Phase I features of *M. polymorpha* are similar to the intense blue light-induced nuclear relocation from the bottom to the side walls in Arabidopsis[1,5,11,12] (see Fig. 4a). Hence, the land colonizer *M. polymorpha* has acquired a primitive ability to respond to intense light, in which nuclei are carried through actin-dependent chloroplast movements that involve MpCHUP1 and MpKAC (Fig. 2j, Phase I).

On the other hand, Phase II is unique to *M. polymorpha* (see Fig. 4a). Phase II involved both actin and microtubules in the movements of nuclei (Fig. 2h) and chloroplasts (Fig. 2i), indicating that the nuclear relocation mechanism in Phase II is different from that in Phase I. Prolonged exposure to intense light may cause desensitization to phototropin as previously reported[13], which would decrease the ability of the nuclei to remain on the side walls. In phase II, the nuclei and chloroplasts positioned on the upper walls directly face the blue light (Fig. 2j, Phase II), which causes UV-induced DNA damage. Therefore, the sun-loving plant Arabidopsis has evolved only Phase I[1]. On the other hand, *M. polymorpha*, which is unable to survive in prolonged intense light[14], thrives in the shade (see Fig. 4b).

Finally, we examined the effect of low light (30 μmol m^{-2} s^{-1}), which has no effect on nuclear relocation in Arabidopsis. When dark-adapted 3-day-old gemmalings, in which most nuclei are on the upper walls, were exposed to low light, their nuclei did not move in a day, but then were gradually relocated to the side walls over several days (Fig. 3a, Extended Data Fig. 4d). These results indicate that *M. polymorpha* has an ability of a long-lasting and

reversible response to low light (Fig. 3e). It should be noted that the conditions of continuous low light exposure for days at a time are impossible in nature.

To clarify the mechanism underlying the nuclear relocation that is unique to *M. polymorpha*, we investigated the effective light quality. Weak irradiation of either blue or red light caused around 40% of the nuclei to relocate to the side walls, while their simultaneous irradiation caused more than 70% of the nuclei to relocate to the side walls (Fig. 3b, Wild type). Consistently, deficiency of phototropin (Mp*phot*^{KO}) caused a defect in the upper-to-side nuclear relocation (Fig. 3b). The upper-to-side relocation that was induced by very low blue light at 1 μmol m^{-2} s^{-1} was enhanced by expression of a constitutively active form of the red-light photoreceptor phytochrome (Mp*phy*^{Y241H}) (Fig. 3b), showing that it was involved in the nuclear relocation. In addition, the low light-induced upper-to-side nuclear relocation was significantly inhibited by latrunculin B and/or oryzalin (Fig. 3c). Collectively, these results show that the low light-induced nuclear relocation in *M. polymorpha* is regulated coordinately by two photoreceptors (phototropin and phytochrome) and two cytoskeletons (actin and microtubules) (Fig. 3e). This is in contrast to the lack of involvement of microtubules and phytochrome in the nuclear relocation in Arabidopsis[6,7].

Both the Mp*chup1*^{KO} and Mp*chup1*^{ld} mutants, which are defective in chloroplast movement, showed no significant defect in nuclear relocation after 3 days of low light exposure, indicating that chloroplast movement contributed minimally to nuclear relocation (Fig. 3d and Extended Data Fig. 4e). This was consistent with the finding that chloroplasts remained on the upper walls in the low light (Fig. 1d). Hence, nuclear positioning in the low light is independent of chloroplast movement. On the other hand, the Mp*kac*^{KO} and Mp*kac*^{ge} mutants showed a significant defect in the low light-induced upper-to-side nuclear relocation (Fig. 3d, Extended Data Fig. 4e). The defect was rescued by expressing Mp*KAC-Citrine* under the control of the native MpKAC promoter (Fig. 3d). These results indicate that MpKAC plays a substantial role in the response to low light and that Mp*KAC-Citrine* is functional in the cells.

In the rescued line, MpKAC-Citrine was distributed near the plasma membrane (Fig. 3f, Extended Data Fig. 5), as recently reported[15]. Notably, MpKAC-Citrine was also observed as speckles along filamentous structures in the cytosol (Fig. 3g). To clarify the relationship

between MpKAC and the cytoskeleton, extracts of the rescued line were subjected to immunoprecipitation with anti-GFP (citrine) antibody. Three independent experiments showed that the pulled-down products gave positive signals on immunoblots with anti-GFP and anti-actin antibodies, but not with anti-tubulin antibody (Fig. 3h). In the pulled-down products, the signal intensity of MpKAC-citrine completely paralleled that of actin (Fig. 3i). These results indicate that MpKAC associates with actin but not with tubulin, as does Arabidopsis KAC1, which functions in the stabilization of actin filaments[9]. Hence, MpKAC regulates low light-induced upper-to-side nuclear relocation by stabilizing actin filaments in *M. polymorpha*.

The present results show a clear between *M. polymorpha* and Arabidopsis: in the dark, *M. polymorpha* positions nuclei on the upper walls of the epidermal cells, whereas Arabidopsis positions them on the bottom walls (Fig. 4a). Positioning nuclei on the bottom wall keeps genetic material farther from external environmental stresses. On the other hand, *M. polymorpha*, an early land plant bryophyte with underdeveloped vascular bundles, lives in damp places for the efficient absorption of water, but such places are also conducive to the growth of pathogens. Because the upper walls of the epidermal cells are the outermost parts of the plant body, the nuclei in these cells are necessarily and directly exposed to various environmental stresses including pathogen infection. The present results show that they are able to respond rapidly to these stresses (Fig. 4b).

Our results provide a conceptual advance in how light-dependent nuclear relocation was acquired in land plants (Fig. 4). As mentioned above, light-dependent nuclear relocation does not occur in charophyte algae (Extended Data Fig. 1), but it has been observed in a bryophyte (this study), a fern and a flowering plant. Hence, light-dependent nuclear relocation appears to have initially developed in bryophytes as a result of terrestrialization and then diverged as land plants evolved and adapted to new environments.

Methods

Plant materials and growth conditions

A male *Marchantia polymorpha* Takaragaike-1 (Tak-1) was used as a wild-type plant. The phototropin mutant (*Mpphot*^{KO})[16], constitutively active mutant for phytochrome ($_{pro}$*EF:MpPHY*^{Y241H})[17], Mp*chup1*-knockout mutant (Mp*chup1*^{KO})[15], Mp*chup1* large-deletion mutant (Mp*chup1*^{ld})[15], Mp*KAC*-knockout mutant (Mp*kac*^{KO})[15], Mp*KAC* genome-edited mutant (Mp*kac*^{ge}), and MpKAC-Citrine-expressing plants had the Tak-1 background. The plants were maintained asexually as previously described[18,19]. Gemmae were grown aseptically on germination medium (one-half-strength Gamborg's B5 salts, 0.025% [w/v] MES-KOH, pH 5.7, and 1% [w/v] agar) at 22 °C under continuous 30 μmol m^{-2} s^{-1} white light conditions, and the 3-day-old gemmalings (the early growth stage of thalli developing from gemmae) were used unless otherwise stated. *Chara corallina* was grown at 25 °C under a 12-h-white light (20 μmol m^{-2} s^{-1})/12-h-dark cycle. The light intensity was measured using a quantum sensor (LI-190SA; LI-COR) or light analyzer (LA-105; NK System).

Generation of MpKAC-Citrine expressing plants

We constructed Mp*KAC-Citrine* for Mp*kac*^{ko} complementation through amplification of the genomic region containing the 2880-bp upstream of the translational initiation site and the coding sequence of Mp*KAC* from Tak-1 gDNA using the primers 5′-AACCAATTCAGTCGACCAAGCCCAGGTGTATATGGA-3′ and 5′-AAGCTGGGTCTAGATATCCATGAGGCTCATCTCCACCAA-3′, subcloned it into pENTR1A between the SalI and EcoRV sites using an In-Fusion HD Cloning Kit (Takara), and transferred it to the destination vector pMpGWB307[20] using Gateway Clonase II Enzyme Mix (Thermo Fisher Scientific). The resulting plasmids were introduced into Mp*kac*^{ko} using the G-AgarTrap method[21].

To construct $_{pro}$Mp*EF1α:*Mp*KAC-Citrine*, we amplified the coding sequence of Mp*KAC* using the primers 5′-AACCAATTCAGTCGACATGGCAGAGAGGAATAGCTGG-3′ and 5′-AAGCTGGGTCTAGATATCCATGAGGCTCATCTCCACCAA-3′, subcloned it into pENTR1A between the SalI and EcoRV sites using the In-Fusion HD Cloning Kit (Takara), and transferred it to the destination vector pMpGWB108. The resulting plasmids were introduced into Tak-1 cells using the G-AgarTrap method[21].

Genome editing of Mp*KAC*

To generate Mp*kac*^{ge} mutants, we edited the Mp*KAC* locus using a CRISPR/Cas9-based

genome-editing system as previously described[22]. pMpGE013 was digested with AarI restriction enzyme. Annealed oligos for MpKAC_gRNA1_f (5′-CTCGTCAAAATTACGCGAGCCACT-3′) and MpKAC_gRNA1_r (5′-AAACAGTGGCTCGCGTAATTTTGA-3′) were ligated into the linearized vector using DNA Ligation Kit Mighty Mix (Takara). The resulting plasmids were introduced into Tak-1 using the G-AgarTrap method[21]. We extracted gDNA from T_1 thalli and analyzed the sequences using PCR and direct sequencing to identify frameshift mutations.

Dark and light treatments

The dark treatment of *M. polymorpha* gemmalings occurred over 2 days unless otherwise stated. *C. corallina* was dark-treated for 1 day. For the analysis of light-induced nuclear relocation, the samples were irradiated with blue (470 nm), green (525 nm), red (660 nm), or far-red (735 nm) light using an LED light source system (IS-mini; CCS). The light intensity was measured using the quantum sensor (LI-190SA; LI-COR) or light analyzer (LA-105; NK System).

Visualization of the nucleus, chloroplast, and MpKAC-Citrine

Epidermal cells near the apical notches of *M. polymorpha* gemmalings and branchlet cells of *C. corallina* were observed using a fluorescence microscope (Axio Scope A1; Zeiss) equipped with a CCD camera (Axiocam 506 color; Zeiss) or confocal microscope (LSM800; Zeiss: SP8; Leica). To visualize the nuclei, the samples were fixed in a buffer solution (50 mM PIPES, 10 mM EGTA, and 5 mM $MgSO_4$, pH 7.0) containing 1% (w/v) glutaraldehyde for 1 h, stained with 1 µg/mL DAPI (Sigma-Aldrich), and diluted in fixation buffer supplemented with 0.03% (v/v) Triton X-100 for 1.5 h. Chloroplasts were visualized with chlorophyll autofluorescence. MpKAC-Citrine was observed without cell fixation.

Inhibitor treatments

Stock solutions [5 mM latrunculin B (actin-depolymerizing agent, Abcam) and 50 mM oryzalin (microtubule-disrupting agent, Sigma-Aldrich] were prepared in dimethyl sulfoxide (DMSO) and diluted to 10 µM with distilled water. To analyze dark-induced nuclear relocation, inhibitors were applied to 3-day-old gemmalings for 12 h in the dark. As controls, 0.2% (v/v) DMSO and 0.02% (v/v) DMSO were used for latrunculin B and oryzalin, respectively. To analyze low light-induced nuclear relocation, gemmae were grown on germination plates supplemented with inhibitors (10 µM) under 30 µmol m^{-2} s^{-1} white light

conditions for 3 days. As a control, gemmalings were grown on germination plates supplemented with 0.2% (v/v) DMSO for latrunculin B or 0.02% (v/v) DMSO for oryzalin. To analyze intense light-induced nuclear relocation, dark-treated gemmalings were treated with inhibitors in the dark for 1 h before 3 h of blue light irradiation. Alternatively, dark-treated gemmalings were irradiated with blue light for 3 h, followed by treatment with inhibitors under blue light for up to 24 h. As a control, 0.22% (v/v) DMSO was used.

Pull-down assay

A pull-down assay was performed using green fluorescent protein (GFP)-Trap agarose (ChromoTek). We homogenized 1 g of 24-d-old MpKAC-Citrine overexpressing plants in buffer containing 137 mM NaCl, 2.7 mM KCl, 10 mM Na_2HPO_4•$12H_2O$, 1.8 mM KH_2PO_4, 0.5 mM EDTA, 0.1% (v/v) Triton X-100, protease inhibitor cocktail (Roche), and 2.5 mM DSP (pH 7.4) and incubated for 30 min at 25 °C. The homogenates were centrifuged at 9100 ×*g* and 4 °C to remove cellular debris. The supernatants were mixed with GFP-Trap Agarose and incubated at 4 °C for 1 h with inverted mixing. After washing the GFP-Trap Agarose three times with buffer containing 50 mM Tris-HCl, 150 mM NaCl, 0.5 mM EDTA, 0.1% (v/v) Triton X-100, and a protein inhibitor cocktail (pH 7.5), immunoaffinity complexes were eluted with sample buffer containing DTT and SDS (Atto).

SDS-PAGE and immunoblot analysis

Protein extracts obtained from the pull-down assay were subjected to SDS-PAGE, followed by immunoblot analysis, as previously described[7]. SDS-PAGE was performed using a conventional 4–15% precast gel (Criterion TGX; Bio-Rad) according to the manufacturer's instructions. Immunoreactive signals were detected using an ECL detection system (GR Healthcare) with anti-GFP antibody (1:5,000; JL-8; Clontech), anti-actin antibody (1:2,000; clone 10-B3; Sigma-Aldrich), anti-microtubule antibody (1:2,000; clone B-5-1-2; Sigma-Aldrich), and ECL anti-mouse IgG horseradish peroxidase-linked whole antibody (1:1,000; GE Healthcare).

Measurement of chloroplasts and cell surface

The areas of the chloroplasts and cell surface (upper cell plane) were measured using Fiji software (version: 2.14.0/1.54h; https://imagej.net/software/fiji/)[23] to evaluate chloroplast movement. Cells of interest were traced on bright-field images, and their outlines were generated at 15 pixels smaller than the original outlines. The region enclosed by the small

outline was defined as the upper surface of the cell, and the number of pixels was counted. Chlorophyll autofluorescence images were binarized using Fiji software, the smaller outlines were adapted to the binarized images, and the number of pixels of chlorophyll autofluorescence within the small outlines was determined. We finally determined the ratio of chlorophyll fluorescence to cell-surface pixels.

Phylogenetic analysis

CHUP1 and *KAC*, as well as their outgroup genes, in *A. thaliana* (At), *Oryza sativa* (Os), *M. polymorpha* (Mp), *Physcomitrella patens* (Pp)[24,25], and *Chara braunii* (Cb) were searched with AtCHUP1 and AtKAC1 using BLASTp on the NCBI website (https://www.ncbi.nlm.nih.gov/). The accession numbers used in phylogenetic analysis were shown in Supplementary Table 1. The gene accession numbers for the Mp genes (Supplementary Table 1) were obtained from MarpolBase (https://marchantia.info/). Multiple alignments were prepared using MAFFT v7.490[26,27], and non-homologous regions were trimmed using trimAl v1.4[28] with the "-gappyout" option. A phylogenetic tree was constructed using the maximum likelihood method with RAxML v8.2.12[29], with 1,000 bootstraps. The evolutionary model parameter was estimated using the "-m PROTGAMMAAUTO" option. The phylogenetic tree was visualized using FigTree v1.4.4 (http://tree.bio.ed.ac.uk/software/figtree/).

Statistical analysis

Statistical analysis and creation plots were done by Microsoft Excel (Microsoft Corporation) and R version 4.1.2 (https://www.R-project.org/)[30] with Rstudio 2024.04.2+764 (http://www.rstudio.com/)[31]. The ratios of nuclear positions were calculated from all cells observed from five individuals in each experiment. The data were plotted as stacked bar graphs or line graphs with Microsoft Excel and the error bars showed 95% confidence interval approximating Gaussian distribution. Comparison between experimental groups were tested by Fisher's exact test with Bonferroni correction. The ratios of chloroplast positions were calculated as follows; for each experimental condition, 10 cells were observed from each individual, for a total of five individuals with 50 cells, and the ratio of chloroplast position was calculated for each cell. The 50 ratio-data obtained for each experiment were plotted as box and violin or line plots with R package ggplot2[32]. Comparison between experimental groups were tested by Mann-Whitney *U*-test with Bonferroni correction. All tests were two tailed, and statistical significance was set at $p < 0.06$.

Data availability statement

Sequence data from this study can be found in MarpolBase data libraries under the following accession numbers: Mp*PHOT* (Mp5g03810), Mp*PHY* (Mp2g16090), Mp*CHUP1* (Mp7g03540), and Mp*KAC* (Mp3g03760). The data that support the findings of this study are available from the corresponding authors upon request.

References

1. Iwabuchi, K., Hidema, J., Tamura, K., Takagi, S. & Hara-Nishimura, I. Plant Nuclei Move to Escape Ultraviolet-Induced DNA Damage and Cell Death. *Plant Physiol*. **170**, 678-685 (2016).
2. Tsuboi, H., Suetsugu, N., Kawai-Toyooka, H. & Wada, M. Phototropins and neochrome1 mediate nuclear movement in the fern *Adiantum capillus-veneris*. *Plant Cell Physiol*. **48**, 892-896 (2007).
3. Kagawa, T. & Wada, M. Light-dependent nuclear positioning in prothallial cells ofAdiantum capillus-veneris. *Protoplasma*. **177**, 82-85 (1993).
4. Kagawa, T. & Wada, M. Polarized light induces nuclear migration in prothallial cells ofAdiantum capillus-veneris L. *Planta*. **196**, 775-780 (1995).
5. Iwabuchi, K., Sakai, T. & Takagi, S. Blue light-dependent nuclear positioning in *Arabidopsis thaliana* leaf cells. *Plant Cell Physiol*. **48**, 1291-1298 (2007).
6. Iwabuchi, K., Minamino, R. & Takagi, S. Actin reorganization underlies phototropin-dependent positioning of nuclei in Arabidopsis leaf cells. *Plant Physiol*. **152**, 1309-1319 (2010).
7. Iwabuchi, K. et al. ANGUSTIFOLIA Regulates Actin Filament Alignment for Nuclear Positioning in Leaves. *Plant Physiol*. **179**, 233-247 (2019).
8. Oikawa, K. et al. Chloroplast unusual positioning1 is essential for proper chloroplast positioning. *Plant Cell*. **15**, 2805-2815 (2003).
9. Suetsugu, N. et al. Two kinesin-like proteins mediate actin-based chloroplast movement in Arabidopsis thaliana. *Proc Natl Acad Sci U S A*. **107**, 8860-8865 (2010).
10. Takagi, S., Islam, M. S. & Iwabuchi, K. Dynamic behavior of double-membrane-bounded organelles in plant cells. *Int Rev Cell Mol Biol*. **286**, 181-222 (2011).
11. Higa, T., Suetsugu, N., Kong, S. G. & Wada, M. Actin-dependent plastid movement is required for motive force generation in directional nuclear movement in plants. *Proc Natl Acad Sci U S A*. **111**, 4327-4331 (2014).
12. Wada, M. Nuclear movement and positioning in plant cells. *Semin Cell Dev Biol*. **82**, 17-24 (2018).
13. Haga, K., Tsuchida-Mayama, T., Yamada, M. & Sakai, T. Arabidopsis ROOT PHOTOTROPISM2 Contributes to the Adaptation to High-Intensity Light in Phototropic Responses. *Plant Cell*. **27**, 1098-1112 (2015).
14. Mache, R. & Loiseaux, S. Light saturation of growth and photosynthesis of the shade plant Marchantia polymorpha. *J Cell Sci*. **12**, 391-401 (1973).
15. Yamamoto-Negi, Y. et al. A kinesin-like protein, KAC, is required for light-induced and actin-based chloroplast movement in Marchantia polymorpha. *Plant Cell Physiol* (2024).
16. Komatsu, A. et al. Phototropin encoded by a single-copy gene mediates chloroplast photorelocation movements in the liverwort Marchantia polymorpha. *Plant Physiol*. **166**, 411-427 (2014).

17. Nishihama, R. et al. Phytochrome-mediated regulation of cell division and growth during regeneration and sporeling development in the liverwort Marchantia polymorpha. *J Plant Res*. **128**, 407-421 (2015).
18. Okada, S. et al. Construction of male and female PAC genomic libraries suitable for identification of Y-chromosome-specific clones from the liverwort, Marchantia polymorpha. *Plant J*. **24**, 421-428 (2000).
19. Takenaka, M. et al. Direct transformation and plant regeneration of the haploid liverwort Marchantia polymorpha L. *Transgenic Res*. **9**, 179-185 (2000).
20. Ishizaki, K. et al. Development of Gateway Binary Vector Series with Four Different Selection Markers for the Liverwort Marchantia polymorpha. *PLoS One*. **10**, e0138876 (2015).
21. Tsuboyama, S., Nonaka, S., Ezura, H. & Kodama, Y. Improved G-AgarTrap: A highly efficient transformation method for intact gemmalings of the liverwort Marchantia polymorpha. *Sci Rep*. **8**, 10800 (2018).
22. Sugano, S. S. et al. Efficient CRISPR/Cas9-based genome editing and its application to conditional genetic analysis in Marchantia polymorpha. *PLoS One*. **13**, e0205117 (2018).
23. Schindelin, J. et al. Fiji: an open-source platform for biological-image analysis. *Nat Methods*. **9**, 676-682 (2012).
24. Suetsugu, N. et al. The KAC family of kinesin-like proteins is essential for the association of chloroplasts with the plasma membrane in land plants. *Plant Cell Physiol*. **53**, 1854-1865 (2012).
25. Usami, H. et al. CHUP1 mediates actin-based light-induced chloroplast avoidance movement in the moss Physcomitrella patens. *Planta*. **236**, 1889-1897 (2012).
26. Katoh, K. & Standley, D. M. MAFFT multiple sequence alignment software version 7: improvements in performance and usability. *Mol Biol Evol*. **30**, 772-780 (2013).
27. Katoh, K., Rozewicki, J. & Yamada, K. D. MAFFT online service: multiple sequence alignment, interactive sequence choice and visualization. *Brief Bioinform*. **20**, 1160-1166 (2019).
28. Capella-Gutierrez, S., Silla-Martinez, J. M. & Gabaldon, T. trimAl: a tool for automated alignment trimming in large-scale phylogenetic analyses. *Bioinformatics*. **25**, 1972-1973 (2009).
29. Stamatakis, A. RAxML version 8: a tool for phylogenetic analysis and post-analysis of large phylogenies. *Bioinformatics*. **30**, 1312-1313 (2014).
30. Team, R. C. R: A language and environment for statistical computing. *R Foundation for Statistical Computing* (2021).
31. Team, R. RStudio: Integrated Development for R. *RStudio, PBC* (2020).
32. Wickham, H. ggplot2: Elegant Graphics for Data Analysis. *Springer-Verlag New York* (2016).

Acknowledgments

We are deeply grateful to Shingo Takagi (Osaka University, deceased on October 28, 2023) for his invaluable suggestions for this study. We are grateful to Yoshiji Okazaki (Osaka Medical and Pharmaceutical University) for the donation of *Chara corallina*. This work was supported by a Grant-in-Aid for Specially Promoted Research (no. 22000014 to I.H.-N.), by Grants-in-Aid for Scientific Research (no. 15H05776 to I.H-.N. and no. 17K15145 to K.I.)

from the Japan Society for the Promotion of Science (JSPS), and by the Hirao Taro Foundation of KONAN GAKUEN for Academic Research to I.H.-N.

Author contributions

Conceptualization, Project administration, Supervision, and Writing; K.I. and I.H.-N.: Investigation and Data curation; K.I.: Formal analysis; K.I. and H.Y.: Visualization; K.I., H.Y., and I.H.-N.: Methodology; Y.W.: Resources; K.C.M., A.K., N.S., Y.S., T.S., R.N., and T.K.: Funding acquisition; K.I., A.H., H.U., and I.H.-N.

Competing interests

The authors declare no competing interests.

Additional information

Extended Data Fig. 1 | Distribution of nuclei in *C. corallina* under dark and light conditions.

Extended Data Fig. 2 | Gemmaling of *M. polymorpha*.

Extended Data Fig. 3 | Phytogenic trees of CHUP1 and KAC proteins.

Extended Data Fig. 4 | Nuclear relocation under dark, low light, and high light conditions**.**

Extended Data Fig. 5 | Intracellular distribution of MpKAC-Citrine in gemmalings.

Supplementary Table 1 | Accession numbers for phylogenetic analysis.

Correspondence and requests for materials should be addressed to Kosei Iwabuchi or Ikuko Har-Nishimura.

Figure legends

Fig. 1 | Dark-induced nuclear relocation depends on two cytoskeletal components in *M. polymorpha*.

a, Representative images of cells from 2-day-dark-treated gemmalings, indicating nuclei stained with DAPI (blue, arrowhead) and chloroplasts (chlorophyll autofluorescence, magenta) located in the upper, middle, and bottom planes of the cells. Scale bar, 20 μm.

b, Three positions of the nucleus in a cell: upper, side, and bottom wall positions.
c, Dark-induced nuclear relocation in the wild-type, Mp*chup1*^{KO}, and Mp*kac*^{KO} mutants. The data represent the ratios of nuclei positioned at the upper, side, and bottom of the cells. Error bars indicate the 95% CI; n = 205–656 cells, five independent experiments.
d, Representative images of cells from 3-day-white-light-grown gemmalings, indicating nuclei stained with DAPI (blue, arrowhead) and chloroplasts (chlorophyll autofluorescence, magenta) located in the upper, middle, and bottom planes of the cells. Scale bar, 20 µm.
e, Time course of dark-induced nuclear relocation. The data represent the ratios of nuclei positioned at the upper, side, and bottom of the cells. Error bars indicate the 95% CI; n = 141–259 cells, five independent experiments.
f, Effect of cytoskeletal inhibitors on dark-induced nuclear relocation. The data represent the ratios of nuclei positioned at the upper, side, and bottom of the cells. Error bars indicate the 95% CI; n = 426–525 cells, five independent experiments.
g, Possible motile systems for dark-induced nuclear relocation in *M. polymorpha* gemmalings.
Different letters above the bars indicate statistically significant difference.

Fig. 2 | Nuclei exhibit two modes of relocation in response to high-intensity blue-light irradiation under the control of different motile systems.
a, Distribution of nuclei under 300 µmol m^{-2} s^{-1} blue-light irradiation. Dark-adapted gemmalings were irradiated with 300 µmol m^{-2} s^{-1} blue light for up to 24 h. Representative images of nuclei stained with DAPI (blue, arrowhead) and chloroplasts (chlorophyll autofluorescence, red). Scale bar, 20 µm.
b, Time course of nuclear relocation under continuous 300 µmol m^{-2} s^{-1} blue light conditions displayed in **a**. The ratios of nuclei positioned at the upper, side, and bottom of the cell are shown. Error bars indicate the 95% CI; n = 457–549 cells, five independent experiments.
c, Time course of chloroplast movement under continuous 300 µmol m^{-2} s^{-1} blue light conditions displayed in **a**. Ratio of chloroplasts on the cell surface are presented in the boxplot; n = 50 cells, five independent experiments.
d, Dependence of nuclear relocation on blue light fluence rate. Dark-adapted gemmalings were irradiated with blue light at 0, 50, 100, 200, 300, 400, and 500 µmol m^{-2} s^{-1} for 3 h. Data represent the ratio of nuclei positioned at the upper, side, and bottom of cells. Error bars indicate the 95% CI; n = 503–602 cells, five independent experiments.
e, Blue light-induced nuclear relocation in the wild-type, Mp*phot*^{KO}, Mp*chup1*^{KO}, Mp*kac*^{KO},

and complementation lines of MpKAC. Dark-adapted gemmalings were irradiated with 300 μmol m^{-2} s^{-1} blue light for 3 h. Data represent the ratio of nuclei positioned at the upper, side, and bottom of cells. Error bars indicate the 95% CI; n = 494–693 cells, five independent experiments.

f, Effects of cytoskeletal inhibitors on blue light-induced nuclear relocation. Dark-adapted gemmalings were irradiated with 300 μmol m^{-2} s^{-1} blue light for 3 h in the presence of either 10 μM latrunculin B, 10 μM oryzalin, or both. Inhibitors were applied to gemmalings 1 h before irradiation. Data represent the ratio of nuclei positioned at the upper, side, and bottom of the cells. Error bars indicate the 95% CI; n = 510–600 cells, five independent experiments.

g, Effects of cytoskeletal inhibitors on blue light-induced chloroplast movement. Dark-adapted gemmalings were irradiated with 300 μmol m^{-2} s^{-1} blue light for 3 h in the presence of either 10 μM latrunculin B, 10 μM oryzalin, or both. Inhibitors were applied to gemmalings 1 h before irradiation. Ratios of chloroplasts on the cell surface are shown in the boxplot and violin plots; n = 50 cells, five independent experiments.

h, Effects of cytoskeletal inhibitors on blue light-induced nuclear relocation. Dark-adapted gemmalings were irradiated with 300 μmol m^{-2} s^{-1} blue light for 24 h in the presence of either 10 μM latrunculin B, 10 μM oryzalin, or both. Inhibitors were applied to gemmalings 3 h after irradiation. Data represent the ratio of nuclei positioned at the upper, side, and bottom of the cells. Error bars indicate the 95% CI; n = 546–678 cells, five independent experiments.

i, Effects of cytoskeletal inhibitors on blue light-induced chloroplast movement. Dark-adapted gemmalings were irradiated with 300 μmol m^{-2} s^{-1} blue light for 24 h in the presence of either 10 μM latrunculin B, 10 μM oryzalin, or both. Inhibitors were applied to gemmalings 3 h after irradiation. Ratios of chloroplasts on the cell surface are shown in the boxplot and violin plots; n = 50 cells, five independent experiments.

j, Possible motile systems for intense light-induced nuclear relocation in *M. polymorpha* gemmalings.

Different letters above the bars indicate statistically significant difference.

Fig. 3 | Low light-induced nuclear relocation requires two photoreceptors and two cytoskeletal components in *M. polymorpha*.

a, Time course of nuclear relocation under low light and dark conditions. The data represent the ratios of nuclei positioned at the upper, side, and bottom of the cells of gemmalings, grown under continuous 30 μmol m^{-2} s^{-1} white light for up to 3 days (left), then in the dark for up to 2 days (middle), and then under continuous 30 μmol m^{-2} s^{-1} white light for up to 5 days

(right). Error bars indicate the 95% CI; n = 115–755 cells, five independent experiments. In the left data, nuclear positions are shown by separating them into two positions (side walls and upper/bottom walls) because we examined gemmae detached from the thalli and it was difficult to distinguish between the upper and bottom wall positions in their small cells. The middle data are the same as in Fig. 1e.

b, Dependence of nuclear relocation on light wavelength and photoreceptors. Over 3 d, gemmae were irradiated with 30 μmol m^{-2} s^{-1} blue or red light or simultaneously with 15 μmol m^{-2} s^{-1} blue and 15 μmol m^{-2} s^{-1} red light; Mp*phot*^{KO} and the wild-type gemmae were simultaneously irradiated with 15 μmol m^{-2} s^{-1} blue and 15 μmol m^{-2} s^{-1} red light; and $_{pro}$*EF:*Mp*PHY*^{Y241H} and the wild-type gemmae were irradiated with 1 μmol m^{-2} s^{-1} blue light. The data represent the ratios of nuclei positioned at the upper, side, and bottom of the cells. Error bars indicate the 95% CI; n = 366–511 cells, five independent experiments.

c, Effects of cytoskeletal inhibitors on low light-induced nuclear relocation. The data represent the ratios of nuclei positioned at the upper, side, and bottom of the cells. Error bars indicate the 95% CI; n = 443–737 cells, five independent experiments.

d, Low light-induced nuclear relocation in the wild-type, Mp*chup1*^{KO}, Mp*kac*^{KO}, and complementation lines of MpKAC. The data represent the ratios of nuclei positioned at the upper, side, and bottom of the cells. Error bars indicate the 95% CI; n = 417–482 cells, five independent experiments.

e, Possible motile systems for low light-induced nuclear relocation in *M. polymorpha* gemmalings.

f,g, Intracellular distribution of MpKAC-Citrine in gemmalings. Cross-section of the middle plane of Mp*kac*^{KO} gemmaling cells expressing MpKAC-Citrine (**f**). MpKAC-Citrine, green; chloroplasts (chlorophyll autofluorescence), magenta. The magnified image of the upper plane is shown in **g**. Scale bars, 20 μm in **f** and 10 μm in **g**.

h, Immunoblot showing the interaction between MpKAC-Citrine and actin. The anti-GFP antibody pull-down products (bound fractions) from three independent experiments on transgenic plants expressing MpKAC-Citrine were subjected to immunoblotting with either anti-tubulin or anti-actin antibodies. M, marker. Signals surrounded by magenta borders are quantified in **j**.

i, Quantification of MpKAC and actin signals exhibiting a strong correlation.

Different letters above the bars indicate statistically significant difference.

Fig. 4 | Evolutionary acquisition and diversification of light- and cytoskeleton-dependent

nuclear relocation in land plants.

a, Comparison of light- and cytoskeleton-dependent nuclear relocation of *M. polymorpha* (see Fig. 1g, Fig. 2j, Fig. 3e) with those of *A. thaliana*[6,7]. Note that the phototropin- and actin-dependent nuclear relocation (Phase I) of *M. polymorpha* is similar to that of *A. thaliana*.

b, Diagram showing our model, in which light-dependent nuclear relocation has initially developed in bryophytes as a result of terrestrialization and then diverged as land plants evolved and adapted to new environments.

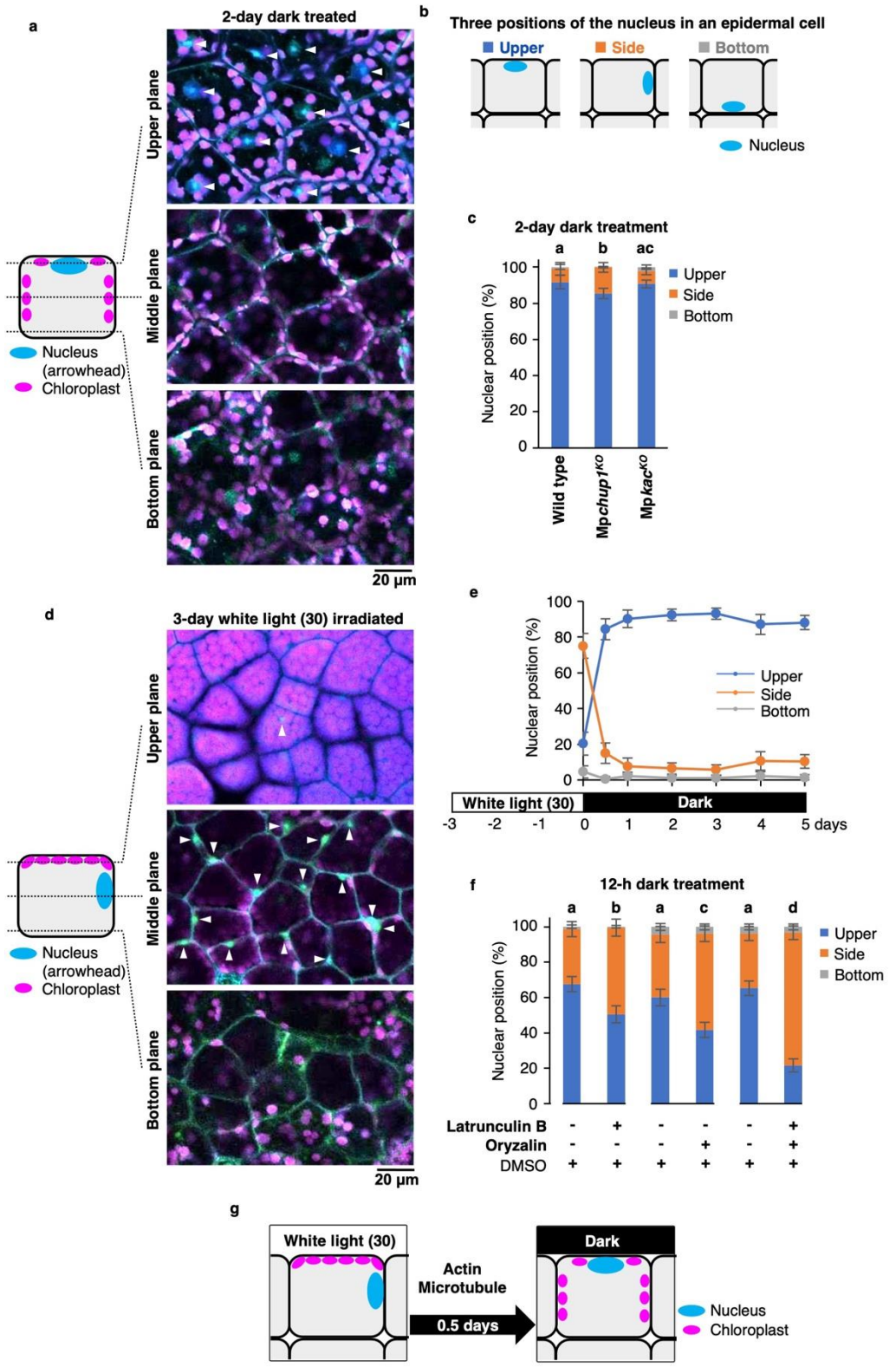

Fig. 1 | Dark-induced nuclear relocation depends on two cytoskeletal components in *M. polymorpha*.
a, Representative images of cells from 2-day-dark-treated gemmalings, indicating nuclei stained with DAPI (blue, arrowhead) and chloroplasts (chlorophyll autofluorescence, magenta) located in the upper, middle, and bottom planes of the cells. Scale bar, 20 µm.
b, Three positions of the nucleus in a cell: upper, side, and bottom wall positions.
c, Dark-induced nuclear relocation in the wild-type, Mp*chup1*^{KO}, and Mp*kac*^{KO} mutants. The data represent the ratios of nuclei positioned at the upper, side, and bottom of the cells. Error bars indicate the 95% CI; n = 205–656 cells, five independent experiments.
d, Representative images of cells from 3-day-white-light-grown gemmalings, indicating nuclei stained with DAPI (blue, arrowhead) and chloroplasts (chlorophyll autofluorescence, magenta) located in the upper, middle, and bottom planes of the cells. Scale bar, 20 µm.
e, Time course of dark-induced nuclear relocation. The data represent the ratios of nuclei positioned at the upper, side, and bottom of the cells. Error bars indicate the 95% CI; n = 141–259 cells, five independent experiments.
f, Effect of cytoskeletal inhibitors on dark-induced nuclear relocation. The data represent the ratios of nuclei positioned at the upper, side, and bottom of the cells. Error bars indicate the 95% CI; n = 426–525 cells, five independent experiments.
g, Possible motile systems for dark-induced nuclear relocation in *M. polymorpha* gemmalings.
Different letters above the bars indicate statistically significant difference.

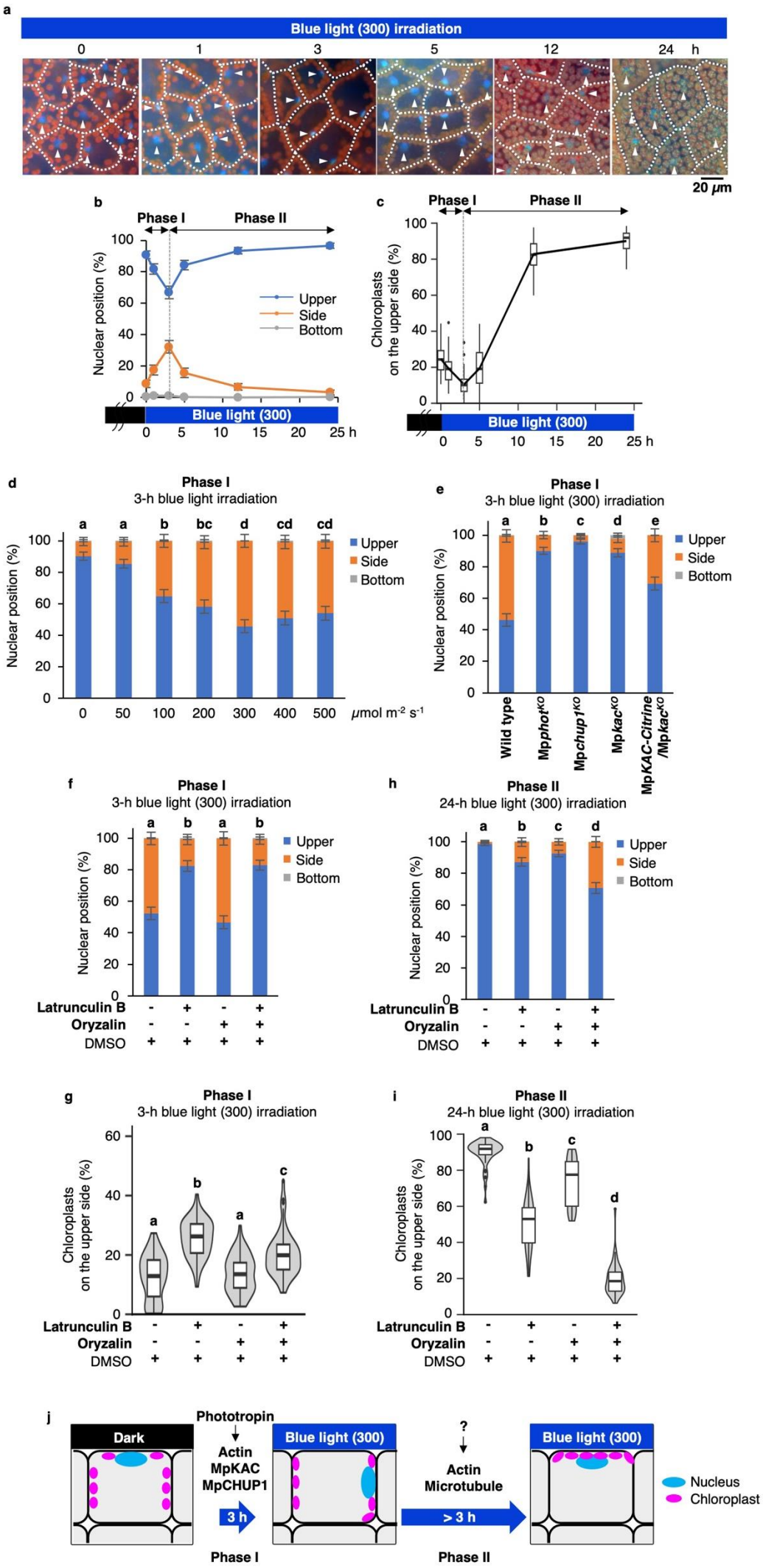
a
Blue light (300) irradiation
0
1
3
5
12
24 h
20 μm
b
Phase I
Phase II
Nuclear position (%)
Upper
Side
Bottom
Blue light (300)
0 5 10 15 20 25 h
c
Phase I
Phase II
Chloroplasts on the upper side (%)
Blue light (300)
0 5 10 15 20 25 h
d
Phase I
3-h blue light irradiation
Nuclear position (%)
a a b bc d cd cd
Upper
Side
Bottom
0 50 100 200 300 400 500 μmol m-2 s-1
e
Phase I
3-h blue light (300) irradiation
Nuclear position (%)
a b c d e
Upper
Side
Bottom
Wild type
MpphotKO
MpchupKO
MpkacKO
MpKAC-Citrine /MpkacKO
f
Phase I
3-h blue light (300) irradiation
Nuclear position (%)
a b a b
Upper
Side
Bottom
Latrunculin B - + - +
Oryzalin - - + +
DMSO + + + +
h
Phase II
24-h blue light (300) irradiation
Nuclear position (%)
a b c d
Upper
Side
Bottom
Latrunculin B - + - +
Oryzalin - - + +
DMSO + + + +
g
Phase I
3-h blue light (300) irradiation
Chloroplasts on the upper side (%)
a b a c
Latrunculin B - + - +
Oryzalin - - + +
DMSO + + + +
i
Phase II
24-h blue light (300) irradiation
Chloroplasts on the upper side (%)
a b c d
Latrunculin B - + - +
Oryzalin - - + +
DMSO + + + +
j
Dark
Phototropin
Actin
MpKAC
MpCHUP1
3 h
Phase I
Blue light (300)
?
Actin
Microtubule
> 3 h
Phase II
Blue light (300)
Nucleus
Chloroplast

Fig. 2 | Nuclei exhibit two modes of relocation in response to intense blue-light irradiation under the control of different motile systems.

a, Distribution of nuclei under 300 µmol m^{-2} s^{-1} blue-light irradiation. Dark-adapted gemmalings were irradiated with 300 µmol m^{-2} s^{-1} blue light for up to 24 h. Representative images of nuclei stained with DAPI (blue, arrowhead) and chloroplasts (chlorophyll autofluorescence, red). Scale bar, 20 µm.

b, Time course of nuclear relocation under continuous 300 µmol m^{-2} s^{-1} blue light conditions displayed in **a**. The ratios of nuclei positioned at the upper, side, and bottom of the cell are shown. Error bars indicate the 95% CI; n = 457–549 cells, five independent experiments.

c, Time course of chloroplast movement under continuous 300 µmol m^{-2} s^{-1} blue light conditions displayed in **a**. Ratio of chloroplasts on the cell surface are presented in the boxplot; n = 50 cells, five independent experiments.

d, Dependence of nuclear relocation on blue light fluence rate. Dark-adapted gemmalings were irradiated with blue light at 0, 50, 100, 200, 300, 400, and 500 µmol m^{-2} s^{-1} for 3 h. Data represent the ratio of nuclei positioned at the upper, side, and bottom of cells. Error bars indicate the 95% CI; n = 503–602 cells, five independent experiments.

e, Blue light-induced nuclear relocation in the wild-type, Mp*phot*^{KO}, Mp*chup1*^{KO}, Mp*kac*^{KO}, and complementation lines of MpKAC. Dark-adapted gemmalings were irradiated with 300 µmol m^{-2} s^{-1} blue light for 3 h. Data represent the ratio of nuclei positioned at the upper, side, and bottom of cells. Error bars indicate the 95% CI; n = 494–693 cells, five independent experiments.

f, Effects of cytoskeletal inhibitors on blue light-induced nuclear relocation. Dark-adapted gemmalings were irradiated with 300 µmol m^{-2} s^{-1} blue light for 3 h in the presence of either 10 µM latrunculin B, 10 µM oryzalin, or both. Inhibitors were applied to gemmalings 1 h before irradiation. Data represent the ratio of nuclei positioned at the upper, side, and bottom of the cells. Error bars indicate the 95% CI; n = 510–600 cells, five independent experiments.

g, Effects of cytoskeletal inhibitors on blue light-induced chloroplast movement. Dark-adapted gemmalings were irradiated with 300 µmol m^{-2} s^{-1} blue light for 3 h in the presence of either 10 µM latrunculin B, 10 µM oryzalin, or both. Inhibitors were applied to gemmalings 1 h before irradiation. Ratios of chloroplasts on the cell surface are shown in the boxplot and violin plots; n = 50 cells, five independent experiments.

h, Effects of cytoskeletal inhibitors on blue light-induced nuclear relocation. Dark-adapted gemmalings were irradiated with 300 µmol m^{-2} s^{-1} blue light for 24 h in the presence of either 10 µM latrunculin B, 10 µM oryzalin, or both. Inhibitors were applied to gemmalings 3 h after irradiation. Data represent the ratio of nuclei positioned at the upper, side, and bottom of the cells. Error bars indicate the 95% CI; n = 546–678 cells, five independent experiments.

i, Effects of cytoskeletal inhibitors on blue light-induced chloroplast movement. Dark-adapted gemmalings were irradiated with 300 µmol m^{-2} s^{-1} blue light for 24 h in the presence of either 10 µM latrunculin B, 10 µM oryzalin, or both. Inhibitors were applied to gemmalings 3 h after irradiation. Ratios of chloroplasts on the cell surface are shown in the boxplot and violin plots; n = 50 cells, five independent experiments.

j, Possible motile systems for intense light-induced nuclear relocation in *M. polymorpha* gemmalings.

Different letters above the bars indicate statistically significant difference.

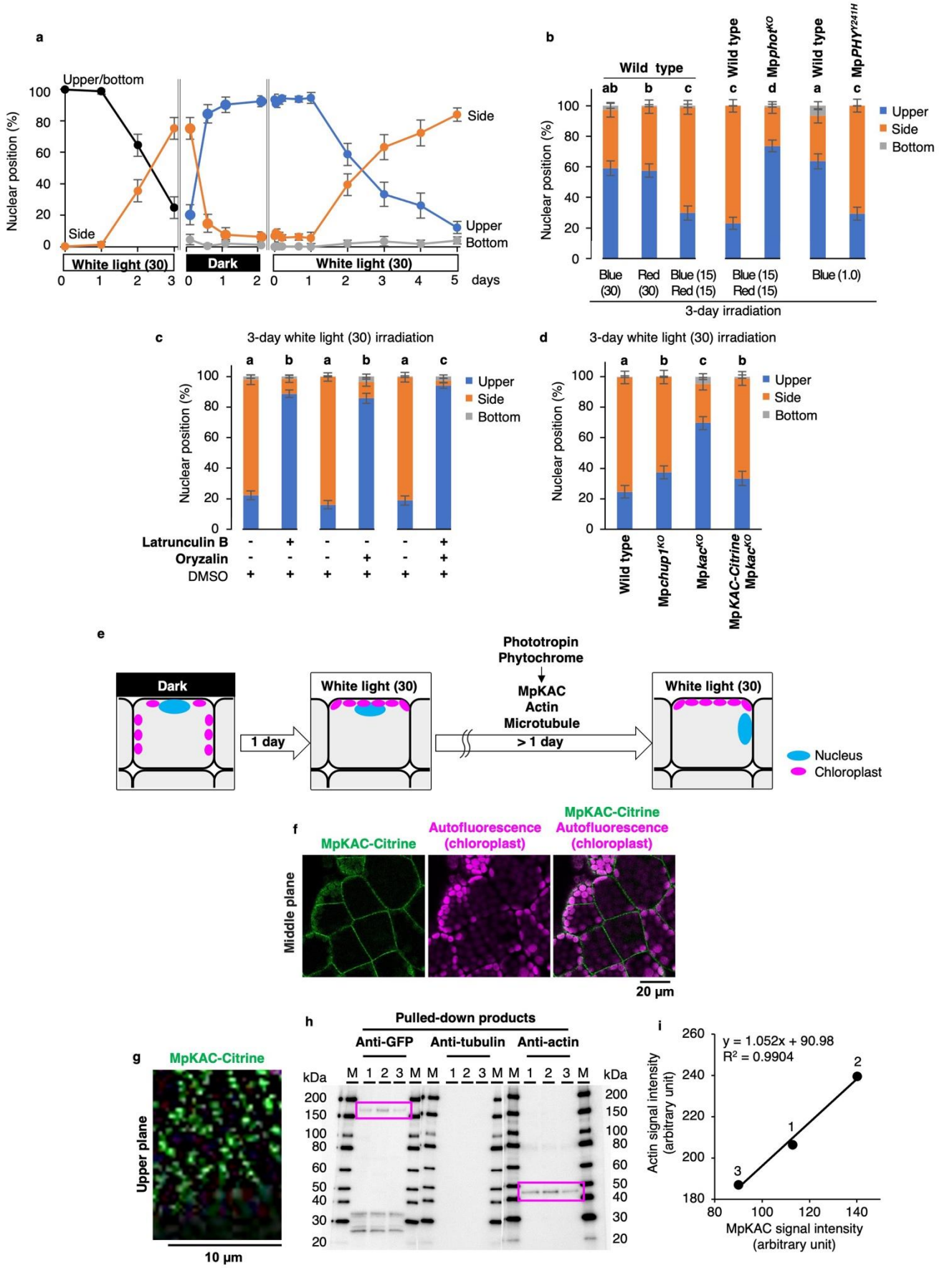
a
Upper/bottom
Side
Nuclear position (%)
White light (30)
Dark
White light (30)
days
Side
Upper
Bottom
b
Wild type
Wild type
MpphotKO
Wild type
MpPHYY241H
Upper
Side
Bottom
Blue (30)
Red (30)
Blue (15) Red (15)
Blue (15) Red (15)
Blue (1.0)
3-day irradiation
c
3-day white light (30) irradiation
Latrunculin B
Oryzalin
DMSO
d
3-day white light (30) irradiation
Wild type
Mpchup1KO
MpkacKO
MpKAC-Citrine MpkacKO
e
Dark
1 day
White light (30)
Phototropin
Phytochrome
MpKAC
Actin
Microtubule
> 1 day
White light (30)
Nucleus
Chloroplast
f
MpKAC-Citrine
Autofluorescence (chloroplast)
MpKAC-Citrine Autofluorescence (chloroplast)
Middle plane
20 µm
g
MpKAC-Citrine
Upper plane
10 µm
h
Pulled-down products
Anti-GFP
Anti-tubulin
Anti-actin
kDa
i
y = 1.052x + 90.98
R² = 0.9904
Actin signal intensity (arbitrary unit)
MpKAC signal intensity (arbitrary unit)

Fig. 3 | Low light-induced nuclear relocation requires two photoreceptors and two cytoskeletal components in *M. polymorpha*.

a, Time course of nuclear relocation under low light and dark conditions. The data represent the ratios of nuclei positioned at the upper, side, and bottom of the cells of gemmalings, grown under continuous 30 µmol m^{-2} s^{-1} white light for up to 3 days (left), then in the dark for up to 2 days (middle), and then under continuous 30 µmol m^{-2} s^{-1} white light for up to 5 days (right). Error bars indicate the 95% CI; n = 115–755 cells, five independent experiments. In the left data, nuclear positions are shown by separating them into two positions (side walls and upper/bottom walls) because we examined gemmae detached from the thalli and it was difficult to distinguish between the upper and bottom wall positions in their small cells. The middle data are the same as in Fig. 1e.

b, Dependence of nuclear relocation on light wavelength and photoreceptors. Over 3 d, gemmae were irradiated with 30 µmol m^{-2} s^{-1} blue or red light or simultaneously with 15 µmol m^{-2} s^{-1} blue and 15 µmol m^{-2} s^{-1} red light; Mp*phot*^{KO} and the wild-type gemmae were simultaneously irradiated with 15 µmol m^{-2} s^{-1} blue and 15 µmol m^{-2} s^{-1} red light; and $_{pro}$*EF:*Mp*PHY*^{Y241H} and the wild-type gemmae were irradiated with 1 µmol m^{-2} s^{-1} blue light. The data represent the ratios of nuclei positioned at the upper, side, and bottom of the cells. Error bars indicate the 95% CI; n = 366–511 cells, five independent experiments.

c, Effects of cytoskeletal inhibitors on low light-induced nuclear relocation. The data represent the ratios of nuclei positioned at the upper, side, and bottom of the cells. Error bars indicate the 95% CI; n = 443–737 cells, five independent experiments.

d, Low light-induced nuclear relocation in the wild-type, Mp*chup1*^{KO}, Mp*kac*^{KO}, and complementation lines of MpKAC. The data represent the ratios of nuclei positioned at the upper, side, and bottom of the cells. Error bars indicate the 95% CI; n = 417–482 cells, five independent experiments.

e, Possible motile systems for low light-induced nuclear relocation in *M. polymorpha* gemmalings.

f,g, Intracellular distribution of MpKAC-Citrine in gemmalings. Cross-section of the middle plane of Mp*kac*^{KO} gemmaling cells expressing MpKAC-Citrine (**f**). MpKAC-Citrine, green; chloroplasts (chlorophyll autofluorescence), magenta. The magnified image of the upper plane is shown in **g**. Scale bars, 20 µm in **f** and 10 µm in **g**.

h, Immunoblot showing the interaction between MpKAC-Citrine and actin. The anti-GFP antibody pull-down products (bound fractions) from three independent experiments on transgenic plants expressing MpKAC-Citrine were subjected to immunoblotting with either anti-tubulin or anti-actin antibodies. M, marker. Signals surrounded by magenta borders are quantified in **j**.

i, Quantification of MpKAC and actin signals exhibiting a strong correlation.

Different letters above the bars indicate statistically significant difference.

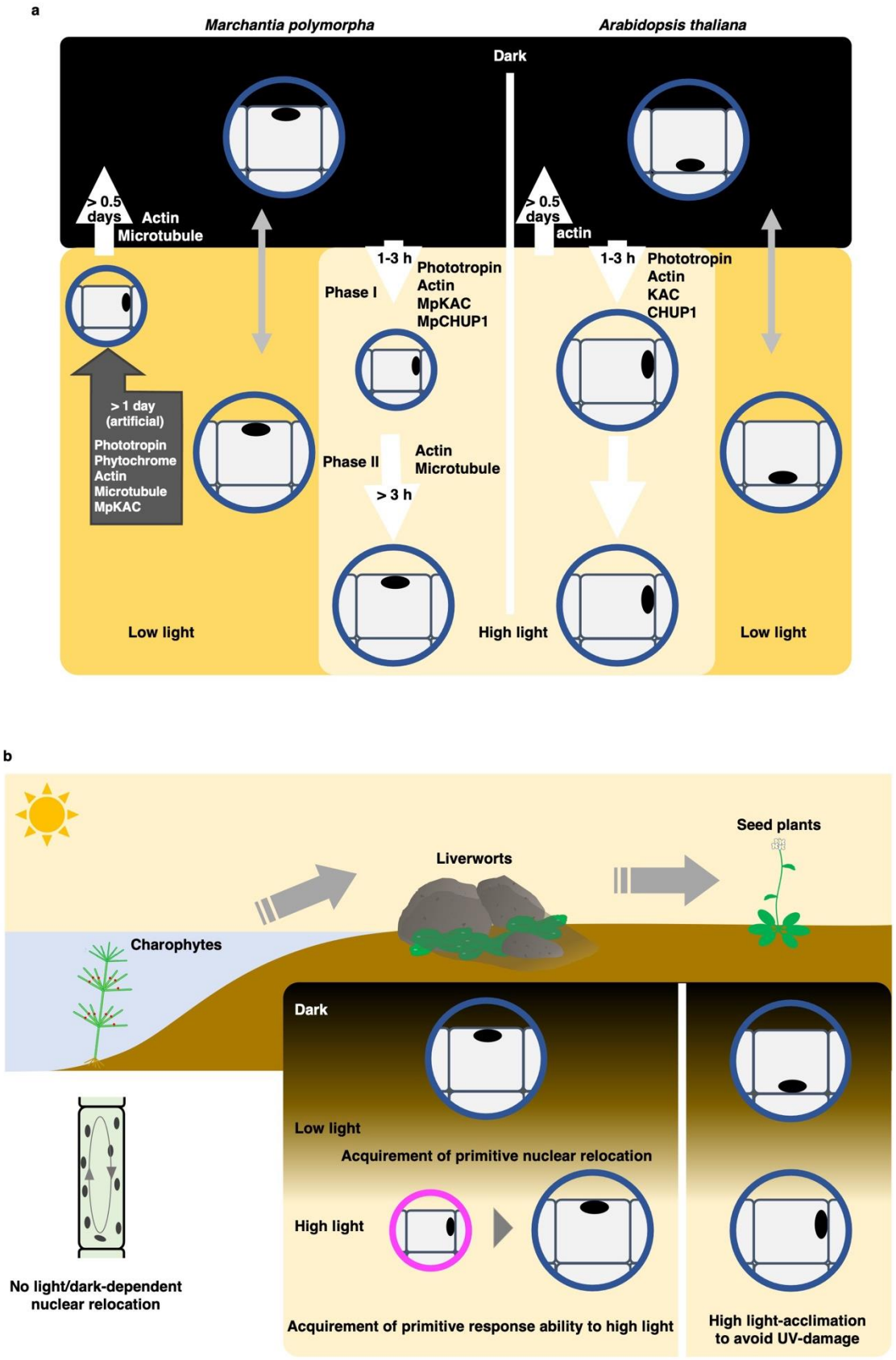

Fig. 4 | Evolutionary acquisition and diversification of light- and cytoskeleton-dependent nuclear relocation in land plants.

a, Comparison of light- and cytoskeleton-dependent nuclear relocation of *M. polymorpha* (see Fig. 1g, Fig. 2j, Fig. 3e) with those of *A. thaliana*[6,7]. Note that the phototropin- and actin-dependent nuclear relocation (Phase I) of *M. polymorpha* is similar to that of *A. thaliana*.

b, Diagram showing our model, in which light-dependent nuclear relocation has initially developed in bryophytes as a result of terrestrialization and then diverged as land plants evolved and adapted to new environments.